JOURNAL

OF THE AMERICAN CHEMICAL SOCIETY

VOLUME 106, NUMBER 4 FEBRUARY 22, 1984

Barriers to Rotation and Inversion in *meso*-1,1′-Bi(2-methylpiperidine)s[1]

Keiichiro Ogawa, Yoshito Takeuchi,* Hiroshi Suzuki, and Yujiro Nomura

Contribution from the Department of Chemistry, The College of Arts and Sciences, The University of Tokyo, Komaba, Meguro-ku, Tokyo, Japan 153. *Received April 15, 1983*

Abstract: A ^{13}C DNMR study of *meso*-1,1-bi(2-methylpiperidine) (**7**), *meso*-1,1′-bi(*cis*-2,4-dimethylpiperidine) (**8**), and *meso*-**1**,1′-bi(*cis*-4-*tert*-butyl-2-methylpiperidine) (**9**) with the aid of molecular mechanics calculation of the corresponding hydrocarbons 1,1′-bi(2-methylcyclohexane) (**14**), 1,1′-bi(*cis*-2,4-dimethylcyclohexane) (**15**), and 1,1′-bi(*cis*-4-*tert*-butyl-2-methylcyclohexane) (**16**) is reported. The most stable conformations of the bipiperidines are the enantiomeric conformations in which the lone pairs of the nitrogen atoms are approximately gauche to each other. In these conformations the N–N bond and all of the alkyl groups are equatorial to each of the chair-form piperidine rings. The energy barriers ($\Delta G^{\ddagger}$) to the interconversion between these enantiomeric gauche conformations in **7**, **8**, and **9** are 12.5 (−25 °C), 17.7 (+72 °C), and 19.0 kcal mol^{-1} (+97 °C), respectively. While the barrier for **7** is assigned to the passing inversion of the nitrogen atoms, the barriers for **8** and **9** are assigned to the single-passing rotation about the N–N bond. In the case of **7**, the next stable conformations, in which one of the methyl groups is axial, were observed at the lower temperatures. The free energy difference between the next stable and the most stable conformations is 0.55 kcal mol^{-1} at −117 °C, and the energy barrier between these conformations is 9.2 kcal mol^{-1} at −82 °C, which is assigned to the ring inversion.

Introduction

Conformational analysis of hydrazines has attracted the interest of physical and organic chemists for more than three decades.[2] Its static aspects have been investigated extensively. It is established that in a simple acyclic alkylhydrazine both of the nitrogen atoms are pyramidal and that in the most stable conformation of such a hydrazine the lone pairs are gauche to each other.[3-5] Its dynamic aspects, however, still lack the elucidation of fundamental problems, one of which is concerned with the energy barrier to nitrogen inversions and that to rotations about the N–N bond.[2,6]

Jones, Katritzky, and co-workers have discovered that there are two types of nitrogen inversions, a passing N-inversion (an inversion that involves eclipsing of one pair of substituents in the transition state) and a nonpassing N-inversion (an inversion that does not involve eclipsing of substituents).[7] The high energy barrier in 1,2-dimethylperhydropyridazines ($\Delta G^{\ddagger} \simeq 12$ kcal mol^{-1})[8] has been interpreted in terms of the passing N-inversion, and the low energy barrier in 1,2-dimethylperhydropyridazines[8] and acyclic alkylhydrazines **1**, **2**, and **3** ($\Delta G^{\ddagger} \simeq 7$–8 kcal mol^{-1})[9]

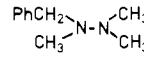

1

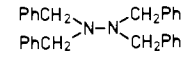

2

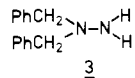

3

has been interpreted in terms of the nonpassing N-inversions.[7] Originally this barrier difference was attributed to the presence or absence of the alkyl substituents passing. Later Nelsen and Weisman pointed out that the barrier difference should be attributed to the difference in the magnitude of the interaction of the lone pairs in the transition state between the two N-inversions.[10] While in the transition state of a passing N-inversion two lone pairs are approximately parallel to each other causing a large repulsive interaction which results in a high barrier; in the transition state of a nonpassing N-inversion, two lone pairs are approximately orthogonal to each other resulting in a low barrier (see Figure 1).

Shvo classified the rotation about the N–N bond into two types, a single-passing rotation (a rotation that involves eclipsing of only

(1) Preliminary reports: Ogawa, K.; Takeuchi, Y.; Suzuki, H.; Nomura, Y. *Chem. Lett.* **1981**, 697; *J. Chem. Soc., Chem. Commun.* **1981**, 1015.

(2) An excellent review of the conformational analysis of hydrazines: Shvo, Y. In "The Chemistry of Hydrazo, Azo, and Azoxy Groups"; Patai, S., Ed.; Interscience: New York, 1975; Part 2, p 1017.

(3) Rademacher, P.; Koopman, H. *Chem. Ber.* **1975**, *108*, 1557. Nelsen, S. F.; Hollised, W. C. *J. Org. Chem.* **1980**, *45*, 3609.

(4) Tanaka, M.; Takeo, H.; Matsumura, C.; Yamanouchi, K.; Kuchitsu, K.; Fukuyama, T. *Chem. Phys. Lett.* **1981**, *83*, 246.

(5) The synthesis of the acyclic hydrazines with the torsion angle of ca. 180°, in which large steric crowding about the N–N bond exists, has been reported. Nelsen, S. F.; Hollinsed, W. C.; Kessel, C. R.; Calabrese, J. C. *J. Am. Chem. Soc.* **1978**, *100*, 7876. Nelsen, S. F.; Gannett, P. M. *Ibid.* **1982**, *104*, 5259.

(6) Lister, D. C.; Macdonald, J. N.; Owen, N. L. "Internal Rotation and Inversion"; Academic Press: London, 1978; Chapter 7.

(7) Jones, R. A. Y.; Katritzky, A. R.; Scattergood, R. *J. Chem. Soc., Chem. Commun.* **1971**, 644. Jones, R. A. Y.; Katritzky, A. R.; Record, K. A. F.; Scattergood, R. *J. Chem. Soc., Perkin Trans. 2* **1974**, 406.

(8) Anderson, J. E. *J. Am. Chem. Soc.* **1969**, *91*, 6374.

(9) Anderson, J. E.; Griffith, D. L.; Roberts, J. D. *J. Am. Chem. Soc.* **1969**, *91*, 637. Dewar, M. J. S.; Jennings, W. B. *Ibid.* **1973**, *95*, 1562.

(10) Nelsen, S. F.; Weisman, G. R. *J. Am. Chem. Soc.* **1976**, *98*, 3281; **1976**, *98*, 7007. Nelsen, S. F. *Acc. Chem. Res.* **1978**, *11*, 14.

0002-7863/84/1506-0831$01.50/0

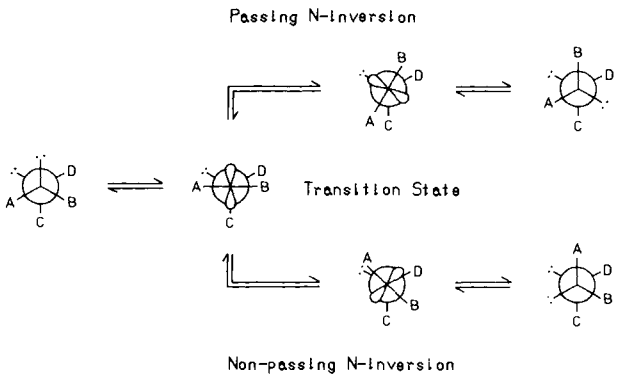

Figure 1. Diagram contrasting lone-pair–lone-pair interactions for the passing (high barrier) and for the nonpassing nitrogen inversion (low barrier), in hydrazine ABN–NCD.

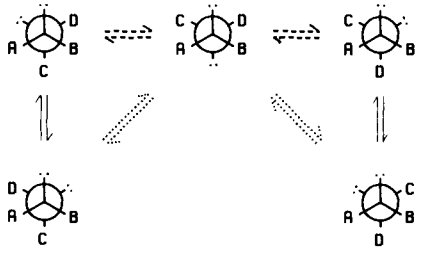

Figure 2. Partial diagram for the conformational interconversion in hydrazine ABN–NCD. A light, a broken, and a dotted arrow represent a nonpassing N-inversion, a passing N-inversion, and a single-passing rotation, respectively.

one pair of substituents in the transition state) and a double-passing rotation (a rotation that involves eclipsing of two pairs of substituents).[11] While in the transition state of a double-passing rotation a passing of lone pairs occurs, in a single-passing rotation a passing of lone pairs does not occur. It is expected that the barrier to a double-passing rotation should be substantially higher than that to a single-passing rotation. This expectation has been supported by an infrared and a microwave spectroscopic study of methylhydrazine[12] and theoretical studies.[13] Rotational barriers of bipyramidal hydrazines other than methylhydrazine have never been determined unambiguously.

Fletcher and Sutherland found the free energy barriers of 10.7–11.2 kcal mol^{-1} for the conformational interconversion in tetraalkylhydrazines **4**, **5**, and **6** by ^{1}H NMR. They assigned these

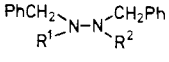

4: $R^1=R^2=Et$
5: $R^1=R^2=iso\text{-}Pr$
6: $R^1=CH_2Ph$, $R^2=Et$

barriers to the "rotation" about the N–N bond.[14] Jones, Katritzky, and co-workers[7] and Shvo,[2] however, have pointed out that the reported barriers can be accounted for by assigning them to the passing N-inversion, as well as by assigning them to the single-passing rotation. The two alternative processes have hitherto never been differentiated in acyclic hydrazines in solution. The difficulty in the differentiation between the two alternatives is that they can

(11) Shvo designated a single-passing rotation and a double-passing rotation as a low-energy rotation and a high-energy rotation, respectively.[2]
(12) Lattimer, R. P.; Harmony, M. D. *J. Am. Chem. Soc.* **1972**, *94*, 351.
(13) Literature through 1973 was cited in ref 2. Riddell, F. G. "The Conformational Analysis of Heterocyclic Compounds"; Academic Press: London, 1980; Chapter 2. Jarvie, J. O.; Rauk, A. *Can. J. Chem.* **1974**, *52*, 2785. Jarvie, J. O.; Rauk, A.; Edmiston, C. K. *Ibid.* **1974**, *52*, 2778. Viktovskaya, N. M.; Dolgunicheva, O. Yu.; Frolov, Yu. L.; Keiko, V. V.; Voronkov, M. G. *Dokl. Akad. Nauk SSSR* **1977**, *235*, 843. Brunk, T. K.; Weinhold, F. *J. Am. Chem. Soc.* **1979**, *101*, 1700. Cowley, A. H.; Mitchell, D. J.; Whangbo, M.-H.; Wolfe, S. *Ibid.* **1979**, *101*, 5224. Chiu, N. S.; Sellers, H. L.; Schafer, L.; Kohata, K. *Ibid.* **1979**, *101*, 5883. Imamura, A.; Ohsaku, M. *Tetrahedron* **1981**, *37*, 2191.
(14) Fletcher, J. R.; Sutherland, I. O. *J. Chem. Soc., Chem. Commun.* **1969**, 706.

Table I. ^{13}C NMR Spectra of *cis*- (**10**) and *trans*-4-*tert*-Butylpiperidine (**11**) in $CDCl_3$

	10				**11**		
position	δ obsd	δ calcd	m[a]	T_1/s	δ obsd	δ calcd	m[a]
2	52.61	53.0	d	4.1	47.46	46.9	d
3	35.86	35.8	t	2.5	32.20	32.9	
4	46.94	46.6		4.2	(40.07)[b]	40.6	
5	27.11	27.2		2.3	28.11	28.1	
6	47.22	47.8		2.4	(40.20)[b]	41.0	
2-CH_3	23.18		q	2.3	17.92		q
$C(CH_3)_3$	32.26		s	17.3	32.14		
$C(CH_3)_3$	27.34			2.1	27.20		q

[a] Multiplicity determined by off-resonance decoupling. [b] Assignments may be exchanged.

bring about the same net conformational interconversion through the same trans conformation (see Figure 2).

We describe here the first successful differentiation between the two alternatives in *meso*-1,1′-bi(2-methylpiperidine) (**7**), *meso*-1,1′-bi(*cis*-2,4-dimethylpiperidine) (**8**), and *meso*-1,1′-bi-(*cis*-4-*tert*-butyl-2-methylpiperidine) (**9**), which leads to the estimation of the barrier to the single-passing rotation, with the aid of ^{13}C DNMR of these compounds and of molecular mechanics calculations of the corresponding hydrocarbons.

Synthesis of Materials. Synthesis of **7** has already been reported.[15] The bipiperidines **8** and **9** were prepared by the silver(I)-catalyzed peroxodisulfate oxidation of the corresponding piperidines (see eq 1). Preparation of *cis*-4-*tert*-butyl-2-

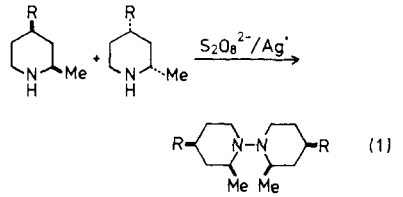

(1)

7: R=H
8: R=Me
9: R=tert-Bu

methylpiperidine (**10**) was accomplished by catalytic hydrogen-

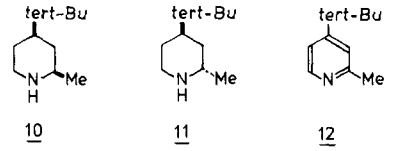

10 **11** **12**

ation of 4-*tert*-butyl-2-methylpyridine (**12**), which was prepared by methylation of 4-*tert*-butylpyridine with methyllithium.

^{13}C NMR Spectra of *cis*- (10) and *trans*-4-*tert*-Butyl-2-methylpiperidine (11). ^{13}C NMR spectra of **10** and **11**, the latter being the byproduct in the catalytic hydrogenation of **12**, are summarized in Table I. Calculated chemical shifts of **10** and **11** were obtained for the 2-methyl equatorial conformation and the 2-methyl axial conformation, respectively, using the parameters of Eliel et al. for methylpiperidines.[16] Effects of the equatorial *tert*-butyl group to the chemical shifts of the ring carbon, which was not included in parameters of Eliel et al. or of Booth et al.,[17] were estimated by comparison of chemical shifts of *tert*-butylcyclohexane (δ 48.4 (C1), 27.7 (C2), 27.3 (C3), 26.7 (C4)[18] with the chemical shift of cyclohexane (δ 26.9);[19] the *tert*-butyl group

(15) Nomura, Y.; Ogawa, K.; Takeuchi, Y.; Tomoda, S. *Chem. Lett.* **1978**, 271. Ogawa, K.; Nomura, Y.; Takeuchi, Y.; Tomoda, S. *J. Chem. Soc., Perkin Trans. 1* **1982**, 3031.
(16) Eliel, E. L.; Kandasamy, D.; Yen, C.; Hargrave, K. D. *J. Am. Chem. Soc.* **1980**, *102*, 3698.
(17) Booth, H.; Griffiths, D. V. *J. Chem. Soc., Perkin Trans. 2* **1973**, 842.
(18) Roberts, J. D.; Weigert, F. J.; Kroschwotz, J. I.; Reich, H. J. *J. Am. Chem. Soc.* **1970**, *92*, 1338.
(19) Burke, J. J.; Lauterbur, P. C. *J. Am. Chem. Soc.* **1964**, *86*, 1870.

Table II. ^{13}C NMR Data for *meso*-1,1'-Bi(2-methylpiperidine)s

	7					8				9			
	solvent = THF-d_8/CS_2 = 5/6 at given temp (°C)					solvent = diglyme-d_{14} at given temp (°C)				solvent = diglyme-d_{14} at given temp (°C)			
	25	−45		−117		146	21			145	48		
signal	δ, m[a]	δ	ass.[b]	δ[c]	int.[d]	δ, m[a]	δ[c]	T_1/s	ass.[b]	δ, m[a]	T_1/s		ass.[b]
C2,2'	57.95, d	58.53	2'	59.29 (59.38)	w	57.51, d	58.23 (57.53)	2.0	2'	58.19, d	58.84	1.8	2'
				58.49 (57.53)	s								
		56.76	2	57.43 (56.44)	w		56.17 (56.44)	1.8	2		56.71	1.4	2
				56.48 (56.44)	s								
C6,6'	48.74, t	55.20	6	55.93 (52.31)	s	*e*	56.35 (52.31)	1.2	6	*e*	56.78	1.1	6
				50.93 (54.19)	w								
		42.11	6'	42.97 (46.78)	s		42.74 (46.78)	1.2	6'		43.19	0.9	6'
				38.25 (46.78)	w								
C3,3'	36.45, t	36.34	*f*	36.65 (36.44)	s	46.38, t	46.01 (44.46)	1.2	*f*	38.77, t	38.47	0.9	*f*
				35.35 (36.44)	w								
		36.17	*f*	36.34 (36.44)	s		45.60 (44.46)	1.2	*f*		38.14	0.9	*f*
				38.25 (36.44)	w								
C5,5'	27.63, t	27.89	*f*	*g*		36.36, t	36.36 (36.44)	1.0	*f*	28.20	28.91	1.0	*f*
				27.78 (28.42)	s								
		27.07	*f*	*g*			35.48 (36.44)	1.1	*f*		38.14	0.9	*f*
				26.93 (28.42)	s								
C4,4'	24.64, t	24.86	*f*	25.46 (26.62)	s	31.84, d	31.94 (33.34)	2.1	*f*	47.74, d	47.59	1.7	*f*
				g									
		24.36	*f*	24.58 (26.62)	s		31.10 (33.34)	1.9	*f*		46.75	1.7	*f*
				g									
2,2'-CH_3	20.37, q	22.36	2	22.84	s	21.41, q	22.54	1.0	2	21.74, q	22.78	1.1	2
				19.79	w								
		19.03	2'	21.17	s		20.78	1.3	2'		20.96	1.2	2'
				11.96	w								
4,4'-CH_3						22.00, q	22.36	1.2	*f*				
							21.95	1.1	*f*				
4,4'-$C(CH_3)_3$										32.40, s	32.36	16.2	*f*
											32.18	*i*	*f*
4,4'-C(CH_3)$_3$										27.78, q	27.67	0.9	*h*

[a] Multiplicity determined by off-resonance decoupling. [b] Assignment referred to the Newman projection of Figure 5. [c] Calculated chemical shft in parentheses. See the text. [d] Signal intensities are classified as strong (s) and weak (w). Peaks s and w correspond to those for G-*SR*eeee (G+*SR*eeee) and G+*SS*eeea (G-*RR*eaee), respectively. [e] The signal still collapsed into the base line. [f] Relative assignments uncertain. [g] The signal was not detected. [h] The signal did not split. [i] T_1 measurements were unsuccessful.

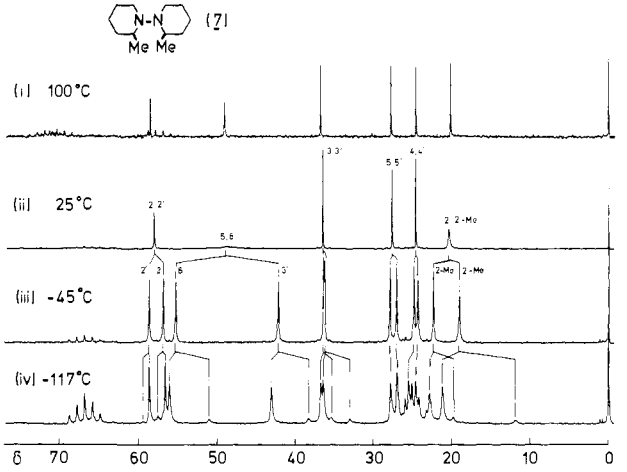

Figure 3. Variable-temperature ^{13}C NMR spectra of *meso*-1,1'-bi(2-methylpiperidine) (**7**): (i) in diglyme-d_{14}; (ii–iv) in THF-d_8/CS_2 = 5/6.

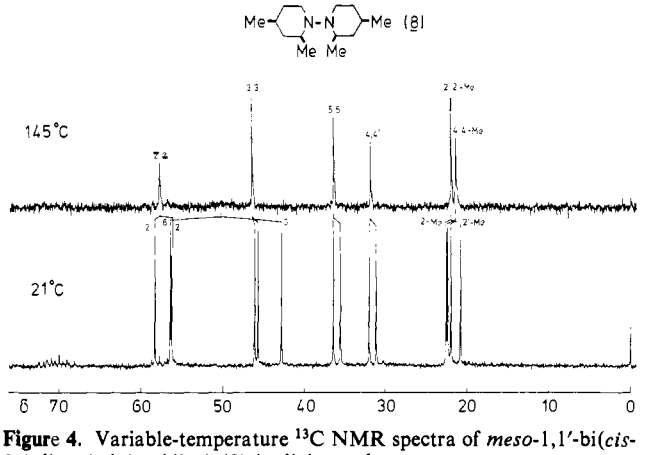

Figure 4. Variable-temperature ^{13}C NMR spectra of *meso*-1,1'-bi(*cis*-2,4-dimethylpiperidine) (**8**) in diglyme-d_{14}.

causes downfield shift of 21.5, 0.8, 0.4, and −0.2 ppm at α, β, γ, and δ positions, respectively. Thus, for **10**,

$$\delta(C2) = 47.61 + 5.04 + 0.4 = 53.05$$

$$\delta(C3) = 27.37 + 7.72 + 0.8 = 35.89$$

$$\delta(C4) = 25.30 - 0.11 + 21.5 = 46.69$$

$$\delta(C5) = 27.37 - 0.92 + 0.8 = 27.25$$

$$\delta(C6) = 47.61 - 0.15 + 0.4 = 47.86$$

Chemical shifts of **11** were calculated in a similar fashion. Agreement of the observed and the calculated chemical shifts is fairly good (within ±0.8 ppm). The peaks for C2, C3, C5, 2-Me, and CMe_3 in **10** and the peaks for C2, C5, 2-Me, and CMe_3 in **11** were assigned from the calculated data, the off-resonance spectra, and/or the signal intensities. Assignment of the peaks for C4 and C6 in **10**, which overlapped each other, was based on the spin–lattice relaxation times T_1, which were measured by the inversion recovery method;[20] the methine carbon C4 (T_1, 4.2 s) and the methylene carbon C6 (T_1, 2.4 s) were clearly differentiated. The peaks for C3 and CMe_3 in **11** were assigned in a similar manner. Thus, on the basis of the analysis of the ^{13}C NMR spectra, the configurations and conformations of **10** and **11** were established.

(20) Vold, R. L.; Waugh, J. S.; Klein, M. P.; Phelps, D. E. *J. Chem. Phys.* **1968**, *48*, 3831. Freeman, R.; Hill, H. D. W. *Ibid.* **1969**, *51*, 3140.

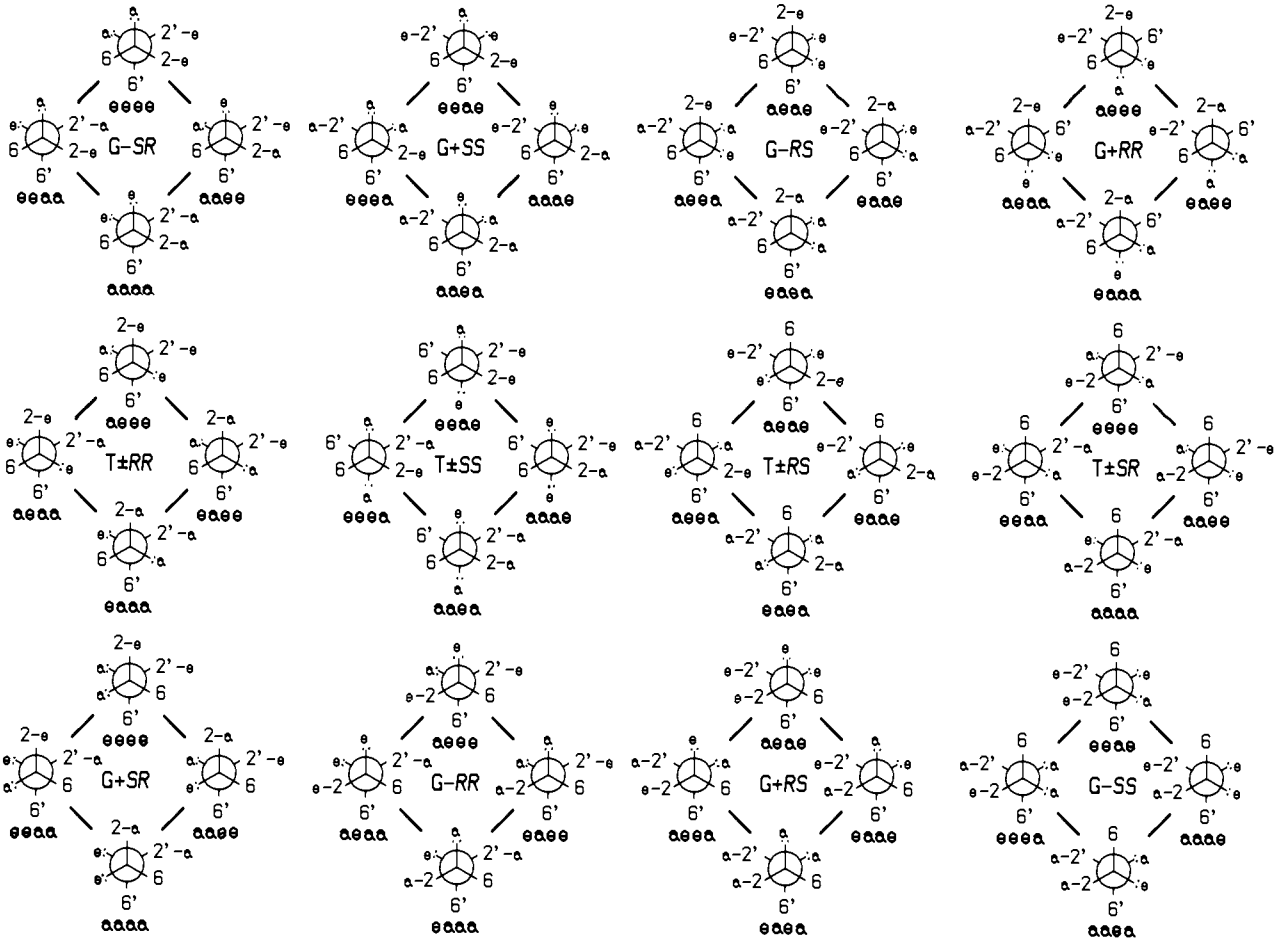

Figure 5. All of the typical gauche and trans conformations in *meso*-1,1′-bi(2-methylpiperidine) (**7**), *meso*-1,1′-bi(*cis*-2,4-dimethylpiperidine) (**8**), and *meso*-1,1′-bi(*cis*-4-*tert*-butyl-2-methylpiperidine) (**9**). Symbol 2-e (2-a) in the Newman projections indicates that the 2-methyl group is equatorial (axial). Symbols 2′-e and 2′-a have analogous meanings for the 2′-methyl group. Symbol e (a) written on a lone pair indicates that the lone pair is equatorial (axial). Heavy lines connecting each of the conformations represent inversions of the piperidine rings.

Variable-Temperature ^{13}C NMR of 7, 8, and 9. The ^{13}C NMR spectra of the three bipiperidines at various temperatures are summarized in Table II. All of the peaks except for those of the methyl carbons of the *tert*-butyl groups split into two peaks of equal intensity as the temperature was lowered (see Figures 3 and 4). For **7**, below −45 °C each of the equally split peaks further splits into two peaks with intensity ratio of ca. 85:15 (see Figure 3). Arguments for the assignment of the signals will appear in later section.

The activation parameters for the rate process were calculated by the total-line-shape analysis (TLS) as well as by the coalescence temperature (T_c) method.[21] They are summarized in Table III. The agreement between $\Delta G^{\ddagger}_c$ values calculated by TLS and those by the T_c method for a rate process is good. Activation parameters obtained from different peaks in one compound agree well.

Discussion

Nomenclature of Conformations. In the bipiperidines the nitrogen inversion (the passing and the nonpassing N-inversion), the rotation about the N–N bond (the single-passing and the double-passing rotation), and the ring inversion operate. All of the typical gauche and trans conformations which are interconvertible by these processes are depicted in Figure 5. We designate conformations in Figure 5 as follows. The first descriptor indicates whether the lone pairs are gauche (G) or trans (T) to each other. The second descriptor represents the sign of the torsion angle of the N–N bond with respect to the lone pairs. We designate these two descriptors as the torsion descriptors. The third and the fourth descriptors represent the configurations of the nitrogen atoms N1 and N1′, respectively. We designate these two descriptors as the configuration descriptors. The fifth descriptor indicates whether the N–N bond is equatorial (e) or axial (a) to the front ring in the Newman projection (ring A). The sixth descriptor indicates whether the 2-methyl group is equatorial (e) or axial (a) to ring A. The seventh descriptor indicates whether the N–N bond is equatorial (e) or axial (a) to the rear ring in the Newman projection (ring B). The last descriptor indicates whether the 2′-methyl group is equatorial (e) or axial (a) to ring B. We designate the last four descriptors as the ring conformation descriptors.

The Most Stable Conformations of 7, 8, and 9. It is established that in the most stable conformation of 1,1′-bipiperidine the lone pair electrons of the nitrogen atoms are approximately gauche to each other (the torsion angle $\simeq 90°$) with the N–N bond equatorial to each of the chair-form piperidine rings.[3] Hence, the most stable conformation of the bipiperidines **7**, **8**, and **9** are certainly the enantiomeric gauche conformations designated as G−*SR*eeee and G+*SR*eeee, in which the N–N bond and all of the alkyl groups are equatorial to each of the piperidine rings, as shown in Figure 5. When the interconversion between the two conformations is fast on the time scale of NMR, the two piperidine units are equivalent and the bipiperidines have an apparent C_2 symmetry. When the interconversion becomes slow, the apparent C_2 symmetry disappears and the signal splittings with the intensity ratio of 1:1 occur. Calculated chemical shifts for G−*SR*eeee (G+*SR*eeee) in **7** and **8** are consistent with the observed chemical shifts (see later section). Hence, the observed rate processes for **7** over −45 °C and for **8** and **9** correspond to the interconversion between G−*SR*eeee and G+*SR*eeee.

Conformational Diagram. In the conformational diagram (Figure 6), each of the conformations is placed at corners of the

(21) Binsch, G. In "Topics in Stereochemistry"; Allinger, N. L., Eliel, E. L., Eds.; Wiley-Interscience: New York, 1968; Vol. 3, p 97. Abraham, R. J.; Loftus, P. "Proton and Carbon-13 NMR Spectroscopy"; Heyden & Son: London, 1978; Chapter 7.

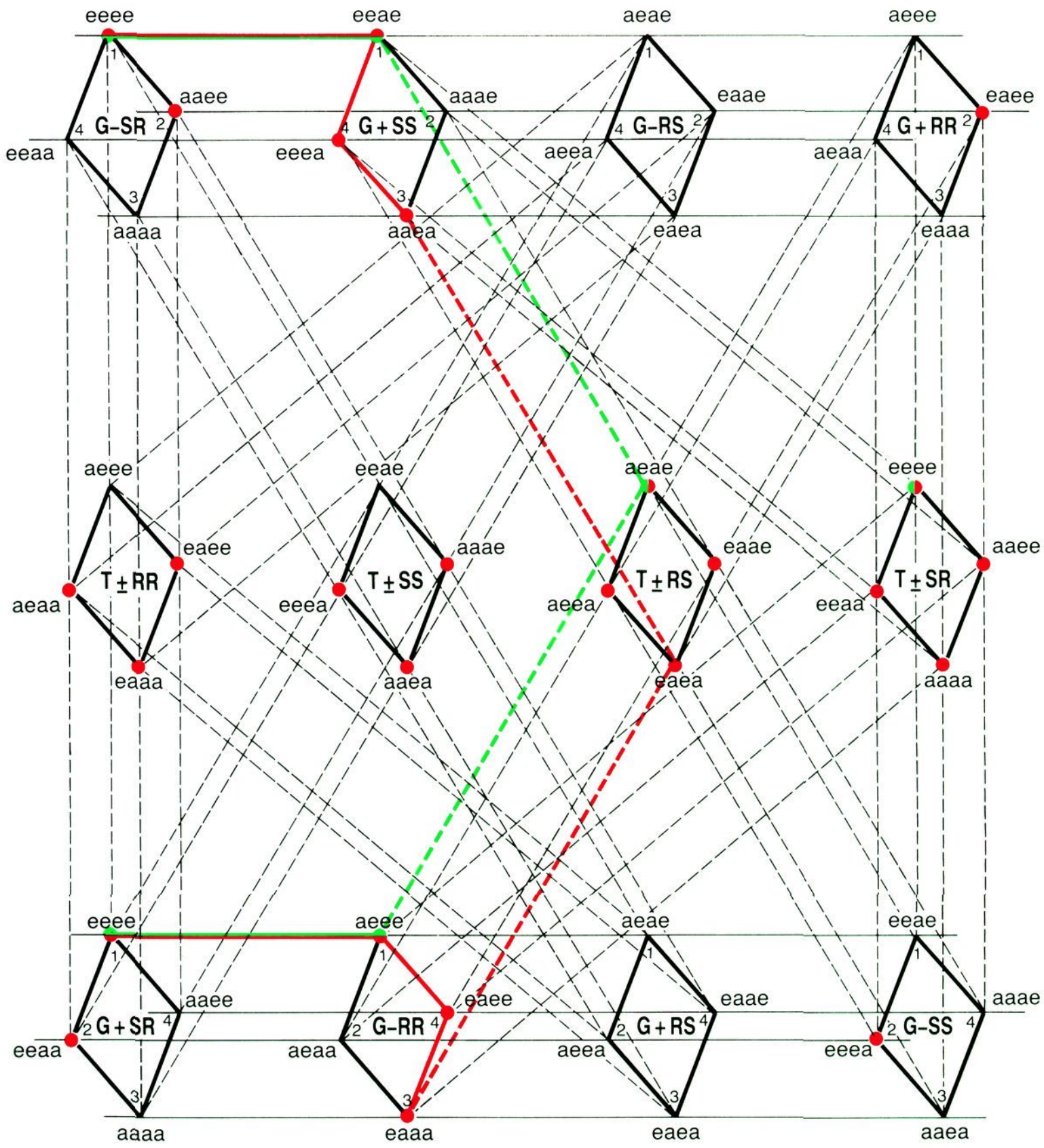

Figure 6. Conformational diagram for *meso*-1,1′-bi(2-methylpiperidine) (**7**), *meso*-1,1′-bi(*cis*-2,4-dimethylpiperidine) (**8**), and *meso*-1,1′-bi(*cis*-4-*tert*-butyl-2-methylpiperidine) (**9**). A light, a broken, and a heavy line represent a nonpassing nitrogen inversion, a passing nitrogen inversion, and a ring inversion, respectively. Red spots represent the sterically possible conformations in **7** and **8**, and red lines represent the lowest barrier inversion paths in these compounds; green spots represent the sterically possible conformation in **9**, and green lines represent the lowest barrier inversion path in this compound.

squares. Each of the squares is designated in terms of the torsion and the configuration descriptors. Conformations on each of the squares are interconvertible by ring inversions, for which the torsion and the configuration descriptors are invariant. An inversion of ring A causes changes of the first two of the ring conformation descriptors. An inversion of ring B causes changes of the last two of the ring conformation descriptors.

Horizontal lines connecting corners of the different squares represent nonpassing N-inversions. Dotted lines connecting corners of different squares represent passing N-inversions. A nonpassing N-inversion causes an interconversion from G to G, and a passing N-inversion causes an interconversion from G to T or from T to G. A nitrogen inversion (passing or nonpassing) of N1 changes the first one of the ring conformation descriptors, and a nitrogen inversion of N1′ changes the third one of the ring conformation descriptors.

Rotational processes are not depicted in the diagram to avoid complication. They can be represented by connecting corners having the same configuration and ring conformation descriptors. Thus the corresponding corners of the following squares are connected by single-passing rotations: G–*SR*,T±*SR*,G+*SR*; G+*SS*,T±*SS*,G–*SS*; G–*RS*,T±*RS*,G+*RS*; G+*RR*,T±*RR*,G–*RR*. Double-passing rotations are given by the following connections: G–*SR*,G+*SR*; G+*SS*,G–*SS*; G–*RS*,G+*RS*; G+*RR*,G–*RR*.

Rotating Newman projections of the gauche conformations in the bottom series by 180° with respect to the axis that bisects the N–N bond orthogonally, we can understand that each of the 16 gauche conformations in the top series has a corresponding enantiomeric gauche conformation in the bottom series. Enantiomeric relationships exist between the same numbered corners of G–*SR* and G+*SR*, between those of *G+SS* and G–*RR*, between those of G–*RS* and G+*RS*, and between those of G+*RR* and *G–SS*. For example, the enantiomer of *G–SR*aaee is *G+SR*eeaa.

Our task is to find the lowest barrier path for the interconversion between G–*SR*eeee and G+*SR*eeee. As stated in the Introduction, the double-passing rotation cannot be involved in the lowest barrier path. Hence, the double-passing rotation is excluded from consideration. As a result, one of the trans conformations must be involved in the interconversion between the two enantiomeric gauche conformations.

Table III. Activation Parameters for Conformational Process in *meso*-1,1'-Bi(2-methylpiperidine)s

compd	signal	line-shape analysis				coalescence-temp analysis				assignment
		temp range[a]	$\Delta H^{\ddagger}$ [b]	$\Delta S^{\ddagger}$ [c]	$\Delta G^{\ddagger}_{298}$ [d]	$\Delta\nu$/Hz	T_c/°C	$\Delta G^{\ddagger}_c$ [d]	$\Delta G^{\ddagger}_c$ [d,e]	
7[f]	C2,2'	−45 to 15	11.86 ± 0.24	−2.93 ± 0.96	12.74 ± 0.05	40.0	−18	12.57 ± 0.05	12.60 ± 0.00	G–*SR*eeee ⇌ G+*SR*eeee
	C3,3'					3.9	−40	12.52 ± 0.10		
	C5,5'	−45 to −1	11.80 ± 0.43	−3.14 ± 1.74	12.67 ± 0.1	18.6	−25	12.60 ± 0.05	12.52 ± 0.00	
	C4,4'					11.2	−29	12.62 ± 0.07		
	2,2'-Me	−41 to 25	11.70 ± 0.22	−3.60 ± 0.81	12.76 ± 0.02	75.2	−10	12.64 ± 0.05	12.64 ± 0.00	
	2-Me	−106 to −55	7.07 ± 0.56	−9.84 ± 3.13	9.90 ± 0.34	210.0	~−82		9.20 ± 0.00	G–*SR*eeee ⇌ G+*SS*eeea and G+*SR*eeee ⇌ G–*RR*eaee
	C6	−106 to −59	6.86 ± 0.79	−11.28 ± 4.11	10.23 ± 0.45	105.5	~−90		8.92 ± 0.02	
8[g]	C3,3'					9.3	62	17.66 ± 0.07		G–*SR*eeee ⇌ G+*SR*eeee
	C5,5'	31 to 103	17.10 ± 0.62	−1.77 ± 1.82	17.64 ± 0.07	20.5	72	17.69 ± 0.05	17.71 ± 0.01	
	C4,4'	31 to 103	17.17 ± 0.67	−1.57 ± 1.98	1.98 ± 0.10	19.5	71	17.66 ± 0.05	17.76 ± 0.01	
9[g]	C4,4'	48 to 145	17.53 ± 0.45	−4.03 ± 1.24	18.74 ± 0.07	19.0	97	19.07 ± 0.07	19.03 ± 0.01	G–*SR*eeee ⇌ G+*SR*eeee
	C3,3'	48 to 95	17.84 ± 0.67	−3.09 ± 1.94	18.76 ± 0.10	7.3	80	18.83 ± 0.10	18.93 ± 0.01	
	2,2'-Me	48 to 145	17.50 ± 0.43	−4.11 ± 1.20	18.74 ± 0.10	41.0	105	18.90 ± 0.05	19.05 ± 0.01	

[a] °C. [b] kcal mol^{-1}. [c] cal K^{-1} mol^{-1}. [d] kcal mol^{-1}. [e] From line-shape analysis. [f] In THF-d_8/CS_2 = 5/6. [g] In diglyme-d_{14}.

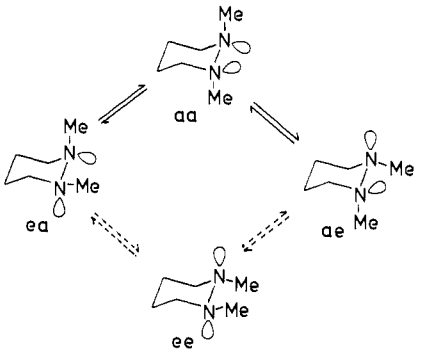

Figure 7. Partial diagram for the conformational interconversion of 1,2-dimethylperhydropyridazine (**13**).[10] A solid and a broken arrow represent a nonpassing and a passing N-inversion, respectively.

Since in the transition state of a nonpassing N-inversion substituents are nearly staggered as shown in Figure 1, the barrier to a nonpassing N-inversion is likely insensitive to steric factors of the substituents. In contrast, the barrier to a passing N-inversion is likely sensitive to steric factors of substituents, since the substituents are nearly eclipsed in its transition state. As stated in the Introduction, the principal cause of the barrier difference between the nonpassing N-inversion and the passing N-inversion is the electronic interaction. The barrier differences between the passing N-inversions, in which the electronic interaction operates equally, must be ascribed to the steric effects. We designate paths for the interconversion that do not involve a single-passing rotation as an inversion path. There are inversion paths that involve ring inversions. The barrier to ring inversions in cyclohexanes and piperidines seems to be insensitive to substituents on the ring and is in the range of 10–13 kcal mol^{-1} ($\Delta G^{\ddagger}$).[22] This value is substantially smaller than our observed barrier values for **8** and **9**. This fact cannot be explained if a ring inversion is the rate-determining step in inversion paths. We assume, therefore, that the transition state of an inversion path lies in a passing N-inversion and that the steric interaction in the transition state is similar to that in the trans conformation involved. This means that the lowest barrier path of inversion paths should involve the trans conformation with the lowest energy. In view of the fact that the interconversion between the most stable conformations ea and ae of 1,2-dimethylperhydropyridazine (**13**) occurs most easily through

13

the less stable conformer aa rather than the more stable conformer ee (see Figure 7),[10] our assumption might appear to be risky. But in the case of **13** the electronic interaction in the transition state is quite different for the two pathways: While the interconversion through aa is the nonpassing N-inversion, that through ee is the passing N-inversion. In contrast, in our case, the electronic interaction is likely approximately equal in all of the inversion paths, since they involve uniformly a passing N-inversion. Therefore, it seems reasonable to assume that the energy of the transition state parallels the steric energy of the trans conformations.

Molecular Mechanics Calculations. The potential energy of the bipiperidines is divided into the steric energy and the electronic energy. The steric energy should be similar to that of the corresponding hydrocarbons, which have C–H bonds in place of the nitrogen lone pairs. The electronic energy largely depends upon the torsion angle of the N–N bond. Hence, the relative stability of conformations with the same torsion angle is considered to be parallel with that of the corresponding hydrocarbons.

(22) Anet, F. A. L.; Anet, R. In "Dynamic Nuclear Magnetic Resonance Spectroscopy"; Jackman, L. M., Cotton, F. A., Eds.; Academic Press: New York, 1975; Chapter 14. Lambert, J. B.; Featherman, S. I. *Chem. Rev.* **1975**, *75*, 611. Katritzky, A. R.; Patel, R. C.; Riddell, F. G. *Angew. Chem., Int. Ed. Engl.* **1981**, *20*, 521.

Table IV. Molecular Mechanics Calculation of the Corresponding Hydrocarbons for the Bipiperidine

		compound[a]					
		14		**15**		**16**	
no.	conformation	torsion angle[b]	energy[c]	torsion angle[b]	energy[c]	torsion angle[b]	energy[c]
1	G–*SR*eece	−78.0	0.00	−78.3	0.00	−77.5	0.00
2	G–*SR*aaee	−57.2	3.97	−64.4	7.56	*d*	*d*
3	G–*SR*aaaa	*d*	*d*	*d*	*d*	*d*	*d*
4	G–*SR*eeaa	*d*	*d*	*d*	*d*	*d*	*d*
5	G+*SS*eeea	89.6	1.15	88.0	4.59	*d*	*d*
6	G+*SS*aaea	90.8	5.24	88.7	12.52	*d*	*d*
7	G+*SS*aaae	*d*	*d*	*d*	*d*	*d*	*d*
8	G+*SS*eeae	58.3	3.51	58.0	3.43	56.7	3.28
9	G–*RS*eaea	*d*	*d*	*d*	*d*	*d*	*d*
10	G–*RS*aeea	*d*	*d*	*d*	*d*	*d*	*d*
11	G–*RS*aeae	*d*	*d*	*d*	*d*	*d*	*d*
12	G–*RS*eaae	*d*	*d*	*d*	*d*	*d*	*d*
13	G+*RR*eaee	64.1	4.29	57.3	7.57	*d*	*d*
14	G+*RR*aeee	*d*	*d*	*d*	*d*	*d*	*d*
15	G+*RR*aeaa	*d*	*d*	*d*	*d*	*d*	*d*
16	G+*RR*eaaa	*d*	*d*	*d*	*d*	*d*	*d*
17	T±*SR*eeee	−178.4	15.78	−178.5	16.16	−178.5	16.81
18	T±*SR*aaee	−179.3	9.05	−179.2	13.08	*d*	*d*
19	T±*SR*aaaa	179.9	4.87	179.9	12.04	*d*	*d*
20	T±*SR*eeaa	179.6	8.74	179.6	12.55	*d*	*d*
21	T±*RR*eaee	−179.0	8.08	−178.8	11.70	*d*	*d*
22	T±*RR*eaaa	180.0	2.62	−179.9	9.56	*d*	*d*
23	T±*RR*aeaa	−179.6	7.43	−179.6	10.92	*d*	*d*
24	T±*RR*aeee	*d*	*d*	*d*	*d*	*d*	*d*
25	T±*RS*eaea	180.0	1.02	180.0	7.94	*d*	*d*
26	T±*RS*aeea	−179.6	5.89	−180.0	8.94	*d*	*d*
27	T±*RS*aeae	180.0	11.05	180.0	10.88	180.0	10.16
28	T±*RS*eaae	179.9	5.58	180.0	8.94	*d*	*d*
29	T±*SS*eeea	179.1	7.51	179.0	11.09	*d*	*d*
30	T±*SS*aaea	−180.0	2.64	179.9	9.56	*d*	*d*
31	T±*SS*aaae	179.6	7.43	179.6	10.94	*d*	*d*
32	T±*SS*eeae	*d*	*d*	*d*	*d*	*d*	*d*

[a] The hydrocarbons **14**, **15**, and **16** correspond to the bipiperidines **7**, **8**, and **9**, respectively (see the text). [b] Torsion angle ω with respect to the H–C1–C1′–H in degrees. [c] Final steric energy in kilocalories per mole. The energies of the most stable conformation G–*SR*eece in each compound (23.48, 23.86, and 36.70 kcal mol^{-1} for **14**, **15**, and **16**, respectively) were set to 0.00 kcal mol^{-1}. [d] Sterically impossible conformation.

We have carried out molecular mechanics calculations (MMI)[23] for the corresponding hydrocarbons 1,1′-bi(2-methylcyclohexane) (**14**), 1,1′-bi(*cis*-2,4-dimethylcyclohexane) (**15**), and 1,1′-bi(*cis*-

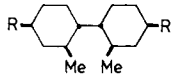

14: R = H
15: R = Me
16: R = tert-Bu

4-*tert*-butyl-2-methylcyclohexane) (**16**) in all of the conformations depicted in Figure 5, since parameters for the N–N bond have not been established. The results are summarized in Table IV. Based on these results, we can roughly estimate the relative stability of the conformations in the bipiperidines. Our statement that the most stable conformations in the bipiperidine are the enantiomeric gauche conformations G–*SR*eeee and G+*SR*eeee has been confirmed also by molecular mechanics calculation.

The Lowest Barrier Inversion Path. The most stable one of the trans conformations in **7** is T±*RS*eaea. Gauche conformations that can directly arrive at T±*RS*eaea by a passing N-inversion are formally G+*SS*aaea, G–*RR*eaaa, G+*RR*eaaa, and G–*SS*aaea. The last two conformations, G+*RR*eaaa and G–*SS*aaea, are sterically impossible conformations. The sterically possible gauche conformation that can directly arrive at G+*SS*aaea (G–*RR*eaaa) is G+*SS*eeea (G–*RR*eaee), which is the next stable gauche conformation. The sterically possible gauche conformation that can arrive at G+*SS*eeea (G–*RR*eaee) is G+*SS*eeae (G–*RR*aeee), which is accessible only from the most stable conformation G–*SR*eeee (G–*SR*eeee). Therefore the lowest barrier inversion path is the following: G–*SR*eeee ⇌ G+*SS*eeae ⇌ G+*SS*eeea ⇌ G+*SS*aaea ⇌ T±*RS*eaea ⇌ G–*RR*eaaa ⇌ G–*RR*eaee ⇌ G–*RR*aeee ⇌ G+*SR*eeee.

The lowest barrier inversion path in **8** is the same inversion path as in **7**: G–*SR*eeee ⇌ G+*SS*eeae ⇌ G+*SS*eeea ⇌ G+*SS*aaea ⇌ T±*RS*eaea ⇌ G–*RR*eaaa ⇌ G–*RR*eaee ⇌ G–*RR*aeee ⇌ G+*SR*eeee.

Among the conformations that are sterically possible for **7** or **8**, those with an axial methyl group are sterically prohibited in the case of **9** since in these conformations the *tert*-butyl group must take the axial position, which is impossible owing to the 1,3-diaxial interaction with the methyl group. As a result, for **9**, there are only two sterically possible trans conformations, T±*RS*aeae and T±*SR*eeee, the former being more stable. Sterically possible gauche conformations that can arrive at T±*RS*aeae are G+*SS*eeae and G–*RR*aeee. G+*SS*eeae (G–*RR*aeee) is accessible only from the most stable conformation G–*SR*eeee (G+*SR*eeee). Hence, the lowest barrier inversion path should be the following: G–*SR*eeee ⇌ G+*SS*eeae ⇌ T±*RS*aeae ⇌ G–*RR*aeee ⇌ G+*SR*eeee.

The Lowest Barrier Rotation Path. We designate a single-passing rotation path G–*SR*eeee ⇌ T±*SR*eeee ⇌ G+*SR*eeee, in which neither nitrogen inversion nor ring inversion is involved, as the pure single-passing rotation path. Energy profiles of the pure single-passing rotation path calculated by MMI for **14**, **15**, **16**, and bi(cyclohexane) (**17**) are shown in Figure 8.[24] The

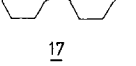

17

(23) Allinger, N. L. Quantum Chemistry Program Exchange, Indiana University, 1975, Program 318.

(24) During the course of our work, Prof. E. Ōsawa has obtained similar results using MM2 for cyclohexylpiperidines: Jaime, C.; Ōsawa, E. *J. Chem. Soc., Chem. Commun.* **1983**, 708; *J. Chem. Soc., Perkin Trans. 2*, in press.

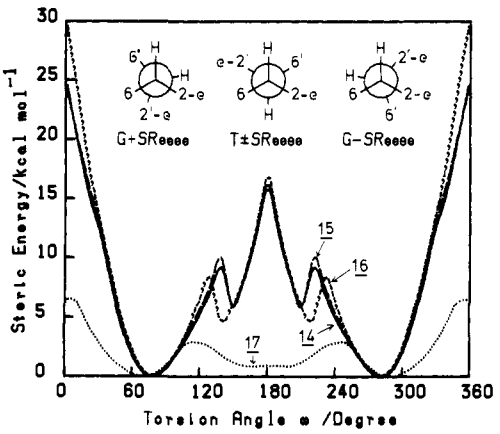

Figure 8. Energy profiles of the bond rotation about the C1–C1′ bond in *meso*-1,1′-bi(2-methylcyclohexane) (**14**) (—), *meso*-1,1′-bi(*cis*-2,4-dimethylcyclohexane) (**15**) (– – –), *meso*-1,1′-bi(*cis*-4-*tert*-butyl-2-methylcyclohexane) (**16**) (----), and bi(cyclohexane) (**17**) (····) calculated by MMI as a function of the torsion angle ω(H–C1–C1′–H). All other internal coordinates are optimized. For **14**, **15**, and **16**, the steric energy of the most stable conformations G–*SR*eeee and G+*SR*eeee in each of the compounds is set to 0.00 kcal mol^{-1} (see note *c* in Table IV). For **17** the minimum of the steric energy (18.31 kcal mol^{-1} at ω = 70.0° and 290.0°) is set to 0.00 kcal mol^{-1}.

important features of the energy profiles are that except in the case of **17** a staggered conformation T±*SR*eeee lies in the saddle point (15.78–16.81 kcal mol^{-1}) and that it is ca. 6–8 kcal mol^{-1} higher than other saddle points (8.35–10.04 kcal mol^{-1}), which correspond to the nearly eclipsed conformations. In Figure 8 the energy of the most stable staggered conformation is taken as the reference. It is known that MMI gives reliable steric energies for staggered conformations of hydrocarbons while it gives lower energies (ca. 10–20% lower) for eclipsed conformations than true values.[25] On the basis of this fact, the steric energies of T±*SR*eeee are expected to be accurate while the steric energies of the nearly eclipsed conformations can be as large as 10.02–12.05 kcal mol^{-1}, which are still lower than T±*SR*eeee. Hence the transition state of the pure single-passing rotation path is certainly T±*SR*eeee. The energies of T±*SR*eeee, i.e., the calculated rotational barriers ($\Delta H^{\ddagger}$) for **14**, **15**, and **16**, are 15.78, 16.16, and 16.81 kcal mol^{-1}, respectively. The experimental rotational barriers for **14**, **15**, and **16** are not known. Theoretical calculations of hydrazine have shown that the trans conformation is a saddle point in the N–N bond rotation owing to the electronic interaction.[13] Hence, in the bipiperidines, both the steric and the electronic effects operate to make T±*SR*eeee a saddle point. The barriers for the pure single-passing rotation path in the bipiperidines are expected to be higher than the calculated rotational barrier for **14**, **15**, and **16**, since the N–N bond is shorter than the C–C bond and since in the bipiperidines there would be repulsive interactions between lone-pair electrons, which do not exist in the hydrocarbons. Although in our first intuition the rotational barrier in **14**, **15**, and **16** are the same, the calculated barriers increase in the order **14**, **15**, **16**. This increase in the calculated rotational barrier can be ascribed to the increase in the rigidity of the molecules.

We designate paths for the interconversion in which nonpassing N-inversion and/or ring inversion are involved in addition to a single-passing rotation as inversion–rotation paths. Since there are impossible gauche and trans conformations, **7** and **8** have only one inversion–rotation path G–*SR*eeee ⇌ G–*SR*aaee ⇌ G+*RR*eaee ⇌ T±*RR*eaee ⇌ G–*RR*eaee ⇌ G–*RR*aeee ⇌ G+*SR*eeee. The inversion–rotation path of **7** and **8** is, however, impossible because of the severe steric congestion at the eclipsed form (the torsion angle ≃120°) between G +*RR*eaee and T±*RR*eaee in the single-passing rotation, which is easily noticed by the inspection of models. For **9**, there is no inversion–rotation path.

Hence, the pure single-passing rotation path is the lowest barrier rotation path.

Table V. Comparison of the Observed Barriers of the Bipiperidines ($\Delta H^{\ddagger}_{obsd}$) with the Calculated Rotational Barriers ($\Delta H^{\ddagger}_{calcd}$) and the Calculated Steric Energies (SE) of the Trans Conformations Involved in the Inversion Paths in the Corresponding Hydrocarbons

bipiperidines		hydrocarbons		
compd	$\Delta H^{\ddagger}_{obsd}$[a,b]	compd	$\Delta H^{\ddagger}_{calcd}$[a,c]	SE[a,d]
7	11.80	**14**	15.78	1.02 (T±*RS*eaea)
8	17.14	**15**	16.16	7.94 (T±*RS*eaea)
9	17.63	16	16.81	10.16 (T±*RS*aeae)

[a] kcal mol^{-1}. [b] From Table III. [c] From Figure 8. [d] From Table IV.

The Inversion Path vs. the Pure Single-Passing Rotation Path. The above discussion has shown that the lowest barrier path for the interconversion between G–*SR*eeee and G+*SR*eeee in each of the bipiperidines is one of two paths, the inversion path or the pure single-passing rotation path. In Table V the observed barriers of the bipiperidines are compared with the calculated steric energies of the trans conformations involved in the inversion paths and the calculated rotational barriers in the corresponding hydrocarbons. Since the observed barrier for **7** ($\Delta H^{\ddagger}$ = 11.8 kcal mol^{-1}) is substantially lower than the calculated barrier to the single-passing rotation path for **14** ($\Delta H^{\ddagger}$ = 15.78 kcal mol^{-1}), the lowest barrier path in **7** is not the rotation path but the inversion path G–*SR*eeee ⇌ G+*SS*eeae ⇌ G+ *SS*eeea ⇌ G+*SS*aaea ⇌ T±*RS*eaea ⇌ G–*RR*eaaa ⇌ G–*RR*eaee ⇌ G–*RR*aeee ⇌ G+*SR*eeee. Hence the observed barrier is assigned to the passing N-inversion between G+*SS*aaea and T±*RS*eaea and between G–*RR*eaaa and T±*RS*eaea.

The difference between the observed barriers of **8** and **9** is much closer to the difference between the calculated rotational barriers of the corresponding hydrocarbons, **15** and **16**, than to the calculated energy difference between T±*RS*eaea of **15** and T±*RS*aeae of **16**. Moreover, the observed barriers of **8** and **9** are slightly higher than the calculated rotational barriers of **15** and **16**. Therefore, we assign the observed barriers of **8** and **9** to the pure single-passing rotation path G–*SR*eeee ⇌ T±*SR*eeee ⇌ G+*SR*eeee. These barriers can be explained by the steric compression that involves a 1,3-diaxial-like interaction between the 2-methyl (2′-methyl) group and the equatorial C6′–H (C6–H) across the N1–N1′ bond. In fact, the energy profile of **17**, which does not have such a steric compression in the trans conformation, shows a minimum with 0.96 kcal mol^{-1} at ω = 180.0° and saddle points with 2.85 kcal mol^{-1} at ω = 120.0° and 240.0° (see Figure 8).[24] The observed barrier for **8** and **9** are well compared with the rotational barrier ($\Delta G^{\ddagger}$ = 17.4 kcal mol^{-1} at −35 °C) of 2,2′-dimethylbiphenyl.[26]

The Lower Temperature Process in 7. The above discussion is further supported by the observation of the lower temperature process in **7**. At lower temperatures all of the peaks of **7** further split into two peaks with intensity ratio of about 85:15. At −117 °C one of the methyl signals splits to a large extent ($\Delta\nu$ = 209.5 Hz) with the weaker peak appearing at higher field (δ 11.9). The weak peak was unequivocally assigned to the axial methyl group from its δ value[27] (see Table II and Figure 3). These results strongly suggest that at the lower temperature the interconversions between G–*SR*eeee and G+*SS*eeea via G+*SS*eeae and between G+*SR*eeee and G–*RR*eaee via G–*RR*aeee are frozen out. From the ratio of the integrated intensities of the axial and the equatorial methyl signals, the free energy of G+*SS*eeea (as well as G–*RR*eaee) was estimated to be higher by 0.55 kcal mol^{-1} at −117 °C than that of G–*SR*eeee (as well as G+*SR*eeee). The calculated

(25) Ōsawa, E.; Shirahama, H.; Matsumoto, T. *J. Am. Chem. Soc.* **1979**, *101*, 4824. Beckhause, H.-D.; Ruchardt, C.; Anderson, J. E. *Tetrahedron* **1982**, *38*, 2299. Ōsawa, E.; Musso, H. In "Topics in Stereochemistry"; Allinger, N. L., Eliel, E. L., Eds.; Wiley-Interscience: New York, 1982; Vol. 13, p 117 and references therein.

(26) Theilacker, W.; Böhm, H. *Angew. Chem., Int. Ed. Engl.* **1967**, *6*, 251.

(27) Wendisch, D.; Feltkamp, H.; Sheidegger, U. *Org. Magn. Reson.* **1973**, *5*, 129.

enthalpy difference between G+*SS*eeea (G–*RR*eaee) and G–*SR*eeee (G+*SR*eeee) in **14** is 1.15 kcal mol^{-1} as shown in Table IV. The entropy contribution due to symmetry of G+*SS*eeea (G–*RR*eaee) is 0 while that of G–*SR*eeee (G+*SR*eeee) is $-R$ ln 2 (1.38 cal/(deg mol)), where R is the gas constant. Hence, the calculated free energy difference in **14** between G+*SS*eeea (G–*RR*eaee) and G–*SR*eeee (G+*SR*eeee) is 0.94 kcal mol^{-1} at −117 °C, which is close to the observed experimental free energy difference in **7**.

In view of the fact that the barriers to the nonpassing N-inversion ($\Delta G^{\ddagger}$ = 7–8 kcal mol^{-1}) in **1**, **2**, and **3** are lower than the barriers to the ring inversion in piperidines ($\Delta G^{\ddagger}$ = 10–13 kcal mol^{-1}), it is concluded that the transition state corresponding to the observed barrier ($\Delta G^{\ddagger}$ = 9.2 kcal mol^{-1} at −117 °C) to the interconversions of **7** between G–*SR*eeee and G+*SS*eeea and between G+*SR*eeee and G–*RR*eaee lies in the ring-inversion processes between G+*SS*eeae and G+*SS*eeea and between G–*RR*aeee and G–*RR*eaee, not in the nonpassing N-inversion processes between G–*SR*eeee and G+*SS*eeae and between G+*SR*eeee and G–*RR*aeee. In other words, it is concluded that the observed barrier is the free energy difference between the transition state of the ring-inversion processes and the most stable conformations G–*SR*eeee and G+*SR*eeee. In **8** and **9** the energy difference between the next most stable conformation G+*SS*eeae (G–*RR*aeee) and the most stable conformation G–*SR*eeee (G+*SR*eeee) is so large that the next most stable conformation was not detected irrespective of the slowing down of the conformational interconversion at lower temperature.

Experimental Section

^{1}H NMR (60-MHz), 90-MHz ^{1}H NMR, and 22.5-MHz ^{13}C NMR spectra were recorded on Jeol 60-HL, Varian EM-390, and Jeol FX90Q spectrometers, respectively. Mass spectra were measured on a Hitachi RMU-6D mass spectrometer. High-resolution mass spectra were measured on a Jeol D300 mass spectrometer. VPC was carried out on a Varian-Aerograph Model 920 instrument with a 20% Triton X-305 column ($^1/_4$ in. × 4 m), on 60–80 mesh Uniport B. Fractional distillation was carried out on a Perkin-Elmer NFT-51 spinning band annular still. Activated alumina powder (200 mesh, Wako Chemicals) was used for the column chromatography.

Materials. *cis*-2,4-Dimethylpiperidine (18).[28] The method of Booth and Little was used for reduction of 3,5-dimethylpyridine.[29] 2,4-Dimethylpyridine (50 g) was dissolved in hot dry EtOH (800 mL) and Na (85 g) was added with magnetic stirring in small pieces at a rate sufficient to maintain boiling. The mixture was cooled, acidified with hydrochloric acid (30%), and heated to remove EtOH under reduced pressure. The residue was basified with aqueous NaOH (40%), and the liberated base was extracted with ether. Distillation gave a colorless oil (45 g), bp 60–67 °C (6.9–7.3 kPa), shown by VPC to contain 58% of *cis*-2,4-dimethylpiperidine (**18**), 10% of the trans isomer, 7% of 1,2,3,6-tetrahydro-2,4-dimethylpyridine, and 24% of 1,2,5,6-tetrahydro-2,4-dimethylpyridine. The mixture (51.5 g), dissolved in dilute HCl (9%, 253 mL), was hydrogenated over Adams platinum oxide catalyst (500 mg) until uptake of hydrogen ceased, and the catalyst was filtered off. This procedure was repeated several times, and the filtrate was gathered. The usual method of recovery gave a mixture (130 g) of *cis*- (77%) and *trans*- (23%) 2,4-dimethylpiperidine from 175 g of 2,4-dimethylpyridine. Fractional distillation (reflux ratio 100, bp 140 °C) gave pure **18** (67 g). Its ^{1}H NMR spectrum was identical with that reported by Wendisch et al.[30] ^{13}C NMR ($CDCl_3$) δ 52.14 (d, C2), 46.96 (t, C6), 43.78 (t, C3), 35.02 (t, C5), 31.55 (d, C4), 23.10 (q, 2-Me), 22.60 (q, 4-Me).

***meso*-1,1'-Bi(*cis*-2,4-dimethylpiperidine) (8).** A 25% aqueous solution of sodium peroxodisulfate (35.7 g, 150 mmol) was added dropwise at 0 °C to a stirred mixture of **18** (11.3 g, 100 mmol), sodium hydroxide (12.0 g, 300 mmol), and a catalytic amount of silver nitrate (850 mg, 5 mmol) in water (120 mL), and the mixture was stirred for additional 3.5 h. After the saturation of the reaction mixture with sodium chloride, it was extracted with ether. The ethereal extract was dried over Na_2SO_4 and concentrated under reduced pressure. The residue was chromatographed 3 times on an alumina column with hexane as an eluant to give *dl*-1,1'-bi(*cis*-2,4-dimethylpiperidine) (**19**) (291 mg, yield 2.6%) and *meso*-1,1'-bi(*cis*-2,4-dimethylpiperidine) (**8**) (140 mg, yield 1.2%), both of which were colorless oils. ^{13}C NMR (THF-d_8/CS_2 = 5/6) of **19** δ 53.70 (d, C2, C2'), 44.19 (t, C6, C6'), 43.26 (t, C3, C3'), 35.22 (t, C5, C5'), 31.77 (d, C4, C4'), 22.39 (q, CH_3), 22.19 (q, CH_3); mass spectrum *m/e* 224 (M^+).

Diastereomeric mixture anal. Calcd for $C_{14}H_{28}N_2$: C, 74.94; H, 12.58; N, 12.49. Found: C, 75.20; H, 12.46; N, 12.34.

4-*tert*-Butyl-2-methylpyridine (12). The method of Ziegler and Zeiser was used for methylation of pyridines.[31] To a stirred solution of methyllithium, prepared from methyl iodide (142 g, 1 mol) and lithium ribbon (17 g, 2.4 mol) in ether,[32] was added 4-*tert*-butylpyridine dropwise for 3.5 h. After 550 mL of dry toluene was added, ether was distilled off, and the solution was refluxed for 14 h. The solution was cooled with an ice bath. The generated lithium hydride and the unchanged methyllithium were decomposed by adding ice into the solution. The solution was acidified with hydrochloric acid (6 N), and the separated water layer was basified with aqueous NaOH (40%). The liberated base was extracted with ether, and the extract was dried over Na_2SO_4 and KOH. Distillation gave a colorless oil (102 g) (bp 101–106 °C (5.3 kPa)), which was shown by VPC, as well as NMR, to contain 63% of 4-*tert*-butyl-2-methylpyridine (**12**) and 37% of unchanged 4-*tert*-butylpyridine. Fractional distillation gave a mixture (40 g) of **12** (90%) and 4-*tert*-butylpyridine (10%), which was used in the catalytic hydrogenation. Preparative VPC and the subsequent distillation gave a colorless oil as an analytically pure sample of **12**. ^{1}H NMR ($CDCl_3$) δ 8.38 (1 H, d, J = 5 Hz), 7.2–6.8 (2 H, m), 2.55 (3 H, s), 1.30 (9 H, s); mass spectrum, *m/e* 149 (M^+).

Anal. Calcd for $C_{10}H_{15}N$: C, 80.48; H, 10.13; N, 9.39. Found: C, 80.53; H, 10.18; N, 9.32.

***cis*-4-*tert*-Butyl-2-methylpiperidine (10).** Raney nickel–aluminum alloy (40%, 4 g) was added slowly to a stirred aqueous solution of sodium hydroxide (20%, 100 mL), which was heated at ca. 50 °C, and it was stirred for an additional 15 min at the same temperature. The supernatant layer was removed by decantation, and the nickel residue was washed with water. To the residue were added *tert*-butyl alcohol (50 mL) and **12** (40 g, contained 10% of 4-*tert*-butylpyridine), and the mixture was heated at 60–70 °C for 1 h with stirring. The catalyst was filtered off, and the filtrate was placed in an autoclave. To the solution were added $Ru(OH)_3$ (600 mg)[33] and $LiOH{\cdot}H_2O$ (100 mg), and the mixture was hydrogenated at 4053 kPa, 80–120 °C. Hydrogen absorption continued for 5 h. THF (50 mL) was added to the mixture, and the solution was filtered through a double layer of $MgSO_4$ and cellulose powder. The filtrate was acidified with hydrochloric acid (10%) and evaporated. The residue was basified with an aqueous solution of NaOH (20%) and was extracted with ether. The extract was dried over $MgSO_4$, concentrated under reduced pressure, and dried again over KOH. Distillation gave 32 g of a colorless oil (bp 92–94 °C (3.7–4.0 kPa)), which was shown by VPC, as well as NMR, to contain 85% of *cis*-4-*tert*-butyl-2-methylpiperidine (**10**), 6% of *trans*-4-*tert*-butyl-2-methylpiperidine (**11**), and 9% of 4-*tert*-butylpiperidine. The distillate was used as the material for the N–N coupling reaction. Preparative VPC gave **10** as a colorless oil and **11** as an easily sublimable, colorless solid (mp 59.0–60.0 °C).

10: ^{1}H NMR ($CDCl_3$) δ 3.25–3.00 (1 H, m), 2.75–2.35 (2 H, m), 1.80–1.45 (3 H, m), 1.4–0.7 (3 H, m), 1.07 (3 H, d, J = 6 Hz), 0.88 (9 H, s); IR (neat) 3250 cm^{-1} (N–H); mass spectrum, *m/e* 155 (M^+).

Anal. Calcd for $C_{10}H_{21}N$: C, 77.35; H, 13.63; N, 9.02. Found: C, 77.22; H, 13.59; N, 8.87.

11: Mass spectrum (high resolution), *m/e* 155.1679 (155.1674 calcd for $C_{10}H_{21}N$); ^{1}H NMR ($CDCl_3$) δ 3.58–3.18 (1 H, br s), 2.95–2.72 (2 H, m), 2.70 (1 H, s), 1.75–1.05 (5 H, m), 1.18 (3 H, d, J = 7 Hz), 0.85 (9 H, s); IR (Nujol) 3410 cm^{-1} (N–H).

***meso*-1,1'-Bi(*cis*-4-*tert*-butyl-2-methylpiperidine) (9).** A 25% aqueous solution of sodium peroxodisulfate (25.0 g, 105 mmol) was added dropwise below 10 °C to a stirred mixture of **10** (a mixture of 85% of **10** and 15% of the trans isomer **11**, 10.8 g, 60 mmol), sodium hydroxide (8.4 g, 210 mmol), and a catalytic amount of silver nitrate (595 mg, 3.5 mmol) in water (84 mL), and the mixture was stirred for an additional 4.5 h. After the reaction mixture was saturated with sodium chloride, it was extracted with ether. The extract was dried over Na_2SO_4 and evaporated under reduced pressure. The residue was chromatographed several times on an alumina column with hexane as the eluant to give *dl*-1,1'-bi(*cis*-4-*tert*-butyl-2-methylpiperidine) (**20**) (89 mg, yield 1%) and the meso isomer (**9**) (40 mg, yield 0.4%).

20: mp 121.0–122.0 °C (needles from MeOH); ^{13}C NMR (THF-d_8) δ 54.81 (d, C2, C2'), 47.68 (t, C4, C4'), 44.04 (t, C6, C6'), 37.21 (t, C3,

(28) Ladenburg, A. *Justus Liebigs Ann. Chem.* **1888**, *247*, 1.
(29) Booth, H.; Little, J. H. *J. Chem. Soc., Perkin Trans. 2* **1972**, 1846.
(30) Feltkamp, H.; Naegele, W.; Wendisch, D. *Org. Magn. Reson.* **1969**, *1*, 11.
(31) Ziegler, K.; Zeiser, H. *Chem. Ber.* **1930**, *63*, 1847. Bohlmann, F.; Englisch, A.; Politt, J.; Sander, H.; Weise, W. *Chem. Ber.* **1955**, *88*, 1831.
(32) Schöllkopf, U.; Paust, J.; Patsch, M. R. "Organic Syntheses"; Wiley: New York, 1973; Collect. Vol. 5; 1973, 859.
(33) Prepared by Professor S. Nishimura.

C3′), 32.49 (s, $C(CH_3)_3$), 28.19 (d, C5, C5′), 27.74 (q, $C(CH_3)$), 21.45 (q, 2-CH_3, 2′-CH_3); mass spectrum, m/e 308 (M^+).

Anal. Calcd for $C_{20}H_{40}N_2$: C, 77.85; H, 13.07; N, 9.08. Found: C, 77.66; H, 12.89; N, 9.07.

9: Mp 94.0–95.0 °C (prisms from MeOH); mass spectrum, m/e 308 (M^+).

Anal. Calcd for $C_{20}H_{40}N_2$: C, 77.85; H, 13.07; N, 9.08. Found: C, 77.80; H, 12.79; N, 8.97.

^{13}C NMR Measurements. All of the variable-temperature ^{13}C NMR spectra were recorded at 22.5 MHz on a Jeol FX90Q spectrometer fitted with a variable-temperature controller Jeol NM-VTS. Typical spectrometer settings are as follows: spectral width 2000 Hz; number of data points, 8K; pulse angle, 55°. The spectrometer was locked on a deuterium signal from THF-d_8 or diglyme-d_{14}. All NMR samples were freeze–thaw degassed and sealed in 10-mm o.d. sample tubes. Temperatures were calibrated with a chromel-alumel thermocouple, which was inserted, at receiver coil height, into another 10-mm o.d. sample tube containing an equal volume of silicone oil. The accuracy of the quoted temperatures is within ±1 °C.

Line-shape calculations were performed on a Hitac M200H computer of Computer Centre University of Tokyo using the programs DNMR3[34] and LSQM2. The spin–spin relaxation time (T_2) was replaced by an effective T_2, which was estimated from the average of the half-height line width of the Me_4Si peak in the whole region of the exchange process. Errors in the enthalpy and entropy of activation are 95% confidence limits from a least-square fit of the Eyring rate equation. Error in the free energy of activation was evaluated from the error of enthalpy and entropy of activation by using the equation of Binsch and Kessler.[35]

In the T_c method, we obtained the free energy of activation at the coalescence temperature from the following equation[21]

$$\Delta G^{\ddagger}_c = RT_c\left[\ln\left(\frac{(2R)^{1/2}}{\pi Nh}\right) + \ln\left(\frac{T_c}{\Delta\nu}\right)\right] \qquad (2)$$

where R is gas constant, T_c the coalescence temperature, N Avogadro constant, and h Planck constant. Errors in $\Delta G^{\ddagger}_c$ (σ_G) were calculated by applying the well-known equation for the propagation of errors[36] to eq 2

$$\sigma_G\ (\mathrm{J\ mol^{-1}}) = \left[\left(\frac{\partial(\Delta G^{\ddagger}_c)}{\partial T_c}\right)^2\sigma_T^2 + \left(\frac{\partial(\Delta G^{\ddagger}_c)}{\partial(\Delta\nu)}\right)^2\sigma_{\Delta\nu}^2\right]^{1/2}$$
$$= 8.3144[[23.96 + \ln(T_c/\Delta\nu)]^2\sigma_T^2 + (T_c/\Delta\nu)^2\sigma_{\Delta\nu}^2]^{1/2}$$

where σ_T is the mean error of T_c in kelvin and $\sigma_{\Delta\nu}$ is the mean error of $\Delta\nu$ in hertz.

The free energy difference between G–*SR*eeee and G+*SS*eeea (or G+*SR*eeee ⇌ G–*RR*eaee) in **7** was determined from the equilibrium constant, which was estimated from the peak area ratio of the split peaks of C6′. It was obtained by cutting and weighing the appropriate portion of the recorded spectra.

Assignment of ^{13}C NMR Signals of 7, 8, and 9. Assignment of the signals in the high-temperature spectra of **7**, **8**, and **9** was made on the basis of the off-resonance spectra and of the similarity between the chemical shifts of the parent piperidine and that of the corresponding 1,1′-bipiperidine.

The assignment of the signals in the high-temperature spectra makes possible the grouping of corresponding resonances at low temperature. Assignment of signals for **7** in the low-temperature (at −117 °C) spectrum rests on comparison of the experimental chemical shifts with calculated ones (Table II), which were obtained by the following procedure: (i) Chemical shifts for the corresponding hydrocarbon **14** in an appropriate conformation were calculated from the parameters of Dalling and Grant, which were derived from perhydroanthracenes and perhydrophenanthrenes,[37] since the ^{13}C chemical shift data of **14** were not available in the literature. (ii) The effects caused by the replacement of two C–H groups by nitrogen atoms were added to the calculated chemical shifts for **14**. We assume that the chemical shift change caused by the replacement of the CH groups by nitrogen atoms in **14** is equal to that caused by the replacement of the CH_2 group by NH in cyclohexane; thus, the chemical shift change of carbon atoms α, β, and γ to the replacement center is 21.4, 1.2, and −0.6 ppm, respectively.[17]

The following example illustrates the procedure for the signal of C2 in conformation G–*SR*eeee. In the analogous conformation of **14** the tertiary C2 carbon (T) has three carbons in α and also three carbons in β position, C2 is involved in three V_g interactions (C3–C2–C1–C6, 2-Me–C2–C1–C1′, C4–C3–C2–C1) and in two V_t interactions (C3–C2–C1–C1′, 2-Me–C2–C1–C6), and the proton attached to C2 is interacting with one of the C6′ protons (γ_{HH}). Hence the predicted chemical shift of the hydrocarbon δ_{BC}(C2) is given by

$$\delta_{BC}(C2) = -2.49 + 3\alpha + 3\beta + T + 3V_g + 2V_t + \gamma_{HH} = 33.84$$

By adding the effect of the CH–N replacement, we obtain the chemical shift of C2 of **7** δ_{BP}(C2):

$$\delta_{BP}(C2) = 33.84 + 21.4 + 1.2 = 56.44$$

In a similar fashion, all of the signals for the ring carbons of G–*SR*eeee and G+*SS*eeea were calculated. In this calculation it is assumed that the effect of a lone pair is equal to that of a C–H bond in γ-gauche steric interactions. Although this seems to be a poor assumption, the magnitude of the interaction between γ-gauche hydrogens (γ_{HH}), which is one of the significant steric interactions, has been proved to be nearly equal to that of the γ-gauche hydrogen and a lone-pair interaction by the examination of the literature data;[10] the chemical shift difference between the 6-axial-CH_3 of 1,2,3,6-tetramethylperhydropyridazine in the conformation **21** (δ 18.74) and that for the 1-axial-CH_3 of 1,2,3,4-tetramethylcyclohexane in the analogous conformation **22** (δ 18.82), which was calculated from the parameters of Dalling and Grant, is negligibly small (0.08).[38] On the basis of the comparison of the calculated with the observed chemical shifts, assignment of the signals for C2, C2′, C6, and C6′ was reliably performed, but the differentiation between the signals for C3 and C3′, C4 and C4′, or C5 and C5′ was unsuccessful since the calculation gives equal values for each set. The assignment of 2-CH_3 and 2′-CH_3 was made considering the γ-gauche steric interaction.

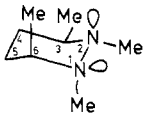

21

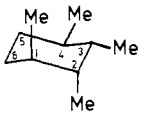

22

Assignment of the signals in the low-temperature spectra of **8** was performed in a similar fashion except in the case of the peaks for C2 and C6, in which the two peaks were so close that they were not differentiated by the inspection of the signal splitting process in the course of temperature variation but clearly differentiated by the measurement of T_1; T_1 of C2′, C2, C6, and C6′ were 2.0, 1.8, 1.2, and 1.2 s, respectively. Assignment of the four peaks for methyl groups in the low-temperature spectrum was made on the basis of the temperature dependence of chemical shifts. Considering steric effects, the larger splitting set was assigned to 2,2′-CH_3 and the smaller splitting set was assigned to 4,4′-CH_3. Thus, assignment of the methyl peaks in the high-temperature spectrum was also accomplished.

In the case of **9**, assignment of the peaks for C2 and C6 in the low-temperature spectrum was similarly made on the basis of the T_1 measurements.

Molecular Mechanics Calculations. Molecular mechanics calculations were carried out with Allinger's MMI program,[23] which was partially modified by the Ōsawa, Kureha group and us without changing the parameters for the force field, on a Hitac M280H of Computer Centre University of Tokyo. In the calculation of each of the gauche conformations in **14**, **15**, and **16** (Table IV), the full-relaxation technique was used, and all structures were optimized without symmetry constraints. The steric energies of the trans conformations (Table IV) and the energy profiles for the rotation about the C1–C1′ bond of **14**, **15**, **16**, and **17** were calculated by using the Wiberg–Boyd bond drive technique.[39]

Acknowledgment. We greatly acknowledge Professor E. Ōsawa of Hokkaido University for offering the program for molecular mechanics calculation MMI and for informing us of his latest results with valuable suggestions. We also thank Dr. A. Tomonaga, Dr. K. Kasai, and Dr. H. Chuman of Kureha Chemical Ind. Co., Ltd., for offering the program ZMMIP for generating coordinate data and the molecular mechanics program MMI and Dr. A. Itai of our university for her help in the use of MMI on a Hitac M-280H computer of Computer Centre University of Tokyo. We are deeply

(34) Kleier, D. A.; Binsch, G. Quantum Chemistry Program Exchange, Indiana University, 1970, Program 165.
(35) Binsch, G.; Kessler, H. *Angew. Chem., Int. Ed. Engl.* **1980**, *19*, 411.
(36) Bevington, P. R. "Data Reduction and Error Analysis for the Physical Science"; McGraw-Hill: New York, 1969; Chapter 4.
(37) Dalling, D. K.; Grant, D. M. *J. Am. Chem. Soc.* **1974**, *96*, 1827.
(38) Dalling, D. K.; Grant, D. M. *J. Am. Chem. Soc.* **1972**, *94*, 5318.
(39) Wiberg, K. B.; Boyd, R. H. *J. Am. Chem. Soc.* **1972**, *94*, 8426.

grateful to Professor M. Ōki of our university for the permission to use DNMR3[34] and LSQM2 programs and for valuable discussions, Professor N. Inamoto of our university for the permission to use the spinning band distillation apparatus, Dr. H. Hirota of our university for the measurements of the high-resolution mass spectra, Professor S. Nishimura of Tokyo University of Agriculture and Technology for his guidance in the catalytic hydrogenation, and The Ministry of Education for the purchase of a Jeol-FX90Q spectrometer. We are also indebted to the referees for valuable suggestions.

Registry No. **7**, 78705-55-2; **8**, 78705-56-3; **9**, 80639-04-9; **10**, 72036-76-1; **11**, 72036-78-3; **14**, 62859-46-5; **15**, 88131-16-2; **16**, 88131-17-3; **17**, 92-51-3.

The Microwave Spectrum, Structure, and Electric Dipole Moment of 1,2,4-Trithiolane

Donald G. Borseth, Kurt W. Hillig II, and Robert L. Kuczkowski*

Contribution from the Department of Chemistry, University of Michigan, Ann Arbor, Michigan 48109. *Received August 8, 1983*

Abstract: The rotational spectra of eight isotopic species of 1,2,4-trithiolane (the sulfur analogue of ethylene ozonide) were assigned and a structure determined by least-squares fitting of the moments of inertia. The molecule has a disulfide-twist half-chair conformation with C_2 symmetry. The structural parameters for the ring atoms are the following: r(S–S) = 2.044 (2) Å, r(C–S_s) = 1.829 (2) Å, r(C–S_d) = 1.808 (2) Å, ∠C–S–S = 93.8 (1)°, ∠C–S–C = 99.4 (1)°, ∠S–C–S = 110.0 (1)°, τ(C–S–S–C) = 52.8 (3)°, τ(S–S–C–S) = 46.4 (4)°, and τ(C–S–C–S) = 20.2 (1.0)°. Vibrational satellites (v = 1–4) from an antisymmetric mode with a fundamental frequency of 82 ± 10 cm^{-1} were observed. A dipole moment of 0.465 (4) D was determined. No effects of fluxional behavior were observed since all the measurements were on vibrational states considerably below the estimated barrier to pseudorotation of 3–6 kcal mol^{-1}.

The structure and conformational properties of disulfides and cyclic disulfides have attracted interest because of the bearing they have on the structure of cystine residues in proteins. Scheraga and co-workers[1] have used vibrational and crystallographic data along with theoretical calculations to obtain insight on changes in properties when the dihedral angle, τ(CS–SC), is varied. Bock and co-workers have investigated the correlation between the photoelectron spectra and dihedral angle[2] and provided an especially extensive study of the fluxionality properties of 1,2-dithiolane[2c] ($\overline{CH_2–CH_2–CH_2–S–S}$) and its radical cation using photoelectron spectroscopy (PES), electron-spin resonance, and ab initio calculations. On the other hand, there has been little gas-phase structural data from microwave (MW) or electron-diffraction studies of cyclic disulfides.

As an outgrowth of our interest in ozonide structures, we undertook a MW study of 1,2,4-trithiolane, $\overline{CH_2–S–S–CH_2–S}$ (sometimes called trithio ozonide), which is the sulfur analogue of ethylene ozonide and the prototype species in the 1,2,4-trithiolane series. Until Morita and Kobayashi[3] provided a reliable synthesis and several bona fide properties in 1967, there was little previous discussion of it in the literature.[4] On the basis of its vibrational and PES spectra,[5] C_2 symmetry has been deduced and a CS–SC dihedral angle of about 50° was estimated. Molecular mechanics calculations[6] have also indicated a twisted conformer with a dihedral angle of about 46° while a flexible conformation and a low barrier to pseudorotation (≤6 kcal mol^{-1}) have been inferred from its proton NMR spectrum[7] which remains a singlet at temperatures down to −117 °C.

More detailed structures are available for three substituted 1,2,4-trithiolanes containing exo-carbon double bonds.[8-10] Species

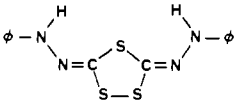

1

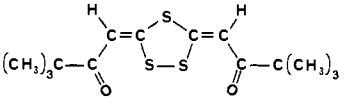

3

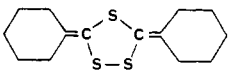

2

(1) (a) Van Wart, H. E.; Shipman, L. L.; Scheraga, H. A. *J. Phys. Chem.* **1975**, *79*, 1428–1436. (b) Van Wart, H. E.; Scheraga, H. A.; *J. Phys. Chem.* **1976**, *80*, 1812–1823. (c) Van Wart, H. E.; Scheraga, H. A.; Martin, R. B. *J. Phys. Chem.* **1976**, *80*, 1832.

(2) (a) Bock, H.; Wagner, G. *Angew. Chem., Int. Ed. Engl.* **1972**, *11*, 150. (b) *Chem. Ber.* **1974**, *107*, 68. (c) Bock, H.; Stein, V.; Semkow, A. *Ibid.* **1980**, *113*, 3208.

(3) Morita, K.; Kobayashi, S. *Chem. Pharm. Bull.* **1967**, *15*, 988.

(4) Breslow, D. S.; Skolnic, H. "The Chemistry of Heterocyclic Compounds"; Weissberger, A., Ed.; Wiley-Interscience: New York, 1966; Vol. 21, Part 1.

(5) (a) Guimon, M. F.; Guimon, C.; Metras, F.; Pfister-Guillouzo, G. *Can. J. Chem.* **1976**, *54*, 146. (b) Guimon, M. F.; Guimon, C.; Pfister-Guillouzo, G. *Tetrahedron Lett.* **1975**, 441.

(6) Allinger, N. L.; Hickey, M. J.; Kao, J. *J. Am. Chem. Soc.* **1976**, *98*, 2741.

(7) Tjan, S. B.; Haakman, J. C.; Teunis, C. J.; Peer, H. G. *Tetrahedron* **1972**, *28*, 3489.

(8) Mellor, J. P.; Nyburg, S. C. *Acta Crystallogr., Sect. B* **1971**, *B27*, 1959.

(9) Casalone, G.; Mugrioli, A. *J. Chem. Soc.* B **1971**, 415.

(10) Winter, W.; Bühl, H.; Meier, H. *Z. Naturforsch., B: Anorg. Chem., Org. Chem.* **1980**, *35B*, 1015.

0002-7863/84/1506-0841$01.50/0